MAJOR ARTICLE

Expression and Role of CXCL10 during the Encephalitic Stage of Experimental and Clinical African Trypanosomiasis

Daniel N. Amin,[1] Martin E. Rottenberg,[2] Allan R. Thomsen,[3] Dieudonné Mumba,[5] Christina Fenger,[4] Krister Kristensson,[1] Philippe Büscher,[6] Bente Finsen,[4] and Willias Masocha[7]

[1]Department of Neuroscience and [2]Microbiology and Tumorbiology Center, Karolinska Institutet, Stockholm, Sweden; [3] Department of International Health, Immunology & Microbiology, University of Copenhagen, Copenhagen, [4]Medical Biotechnology Center, Institute of Medical Biology, University of Southern Denmark, Odense, Denmark; [5]Institut National de Recherche Biomédicale, Kinshasa, Democratic Republic of the Congo; [6]Institute of Tropical Medicine, Department of Parasitology, Antwerp, Belgium; and [7]Department of Applied Therapeutics, Faculty of Pharmacy, Kuwait University, Safat, Kuwait

Background. Human African trypanosomiasis, caused by *Trypanosoma brucei,* involves an early hemolymphatic stage followed by a late encephalitic stage.

Methods. We studied the expression of chemokines with use of microarray and enzyme-linked immunosorbent assay in *T. brucei brucei*–infected mice and in patients with human African trypanosomiasis and examined their role in controlling brain accumulation of T cells and parasites.

Results. The messenger RNAs (mRNAs) encoding CXCR3 ligands CXCL9 and CXCL10 demonstrated the greatest increases among chemokines in brain specimens of infected mice, as determined by microarray. CXCL9 and CXCL10 mRNA accumulation was interferon (IFN)-γ–dependent. Expression of CXCL10 was predominantly observed in astrocytes. Weight loss was registered in wild-type but not in $CXCL10^{-/-}$ and $CXCR3^{-/-}$ infected mice. Infected $CXCL10^{-/-}$ or $CXCR3^{-/-}$ mice demonstrated reduced accumulation of trypanosomes and T cells in the brain parenchyma but similar parasitemia levels, compared with wild-type mice. CXCL10 and IFN-γ levels were increased in the cerebrospinal fluid of patients with late stage but not early stage human African trypanosomiasis. Levels of CXCL10 in patients with late stage human African trypanosomiasis were associated with somnolence, low body weight, and trypanosomes in the cerebrospinal fluid.

Conclusion. IFN-γ–dependent CXCL10 is critical for accumulation of T cells and trypanosomes in the brain during experimental African trypanosomiasis. Data suggest CXCL10 as a candidate marker for late stage human African trypanosomiasis .

Human African trypanosomiasis (HAT), caused by subspecies of *Trypanosoma brucei* that are spread by tsetse fly, is endemic in sub-Saharan Africa. An early hemolymphatic stage of the infection is followed by a meningo-encephalitic stage, in which trypanosomes and/or increased numbers of leukocytes are found in the cerebrospinal fluid (CSF) [1–4]. Toxic arsenic compounds are widely used for treatment of patients with late stage infection, which is invariably fatal if untreated. In rodent models of brain infection, trypanosomes accumulate early after infection in the choroid plexus and circumventricular organs, which have blood vessels permeable to macromolecules. Only at later time points do the parasites penetrate across the blood-brain barrier into the brain parenchyma, in spite of several preceding waves of parasitemia [5, 6]. The penetration of leukocytes and parasites into the brain parenchyma probably underlie the morbidity of the late stage of infection [7].

Chemokines mediate the recruitment and retention of immune cells in inflamed tissues. In addition to their important role in inflammation, chemokines are in-

Received 13 December 2008; accepted 3 March 2009; electronically published 14 October 2009.

Potential conflicts of interest: none reported.

Presented in part: Infectious Diseases of the Nervous System: Pathogenesis and Worldwide Impact Conference, Paris, France, September 2008.

Financial support: European Union (FP6-2004-INCO-DEV-3 032324; NEUROTRYP); International Brain Research Organisation (post-doctoral research fellowship to D.N.A.); Belgian Directorate General for Development Co-operation (PhD grant to D.M.).

Reprints or correspondence: Willias Masocha, Dept of Applied Therapeutics, Faculty of Pharmacy, Kuwait University, PO Box 24923 Safat, 13110 Kuwait (masocha@hsc.edu.kw).

The Journal of Infectious Diseases 2009; 200:1556–65

0022-1899/2009/20010-0011$15.00
DOI: 10.1086/644597

volved in a number of immune processes, including regulation of lymphocyte differentiation and immune surveillance, by controlling the migration of cells into and from secondary lymphoid organs [8].

Individual chemokines play opposing roles in neuroinflammation in different experimental models of infectious disease, making it difficult to predict whether chemokines are protective by contributing to immune eradication of the microbial attack or are causing inflammatory damage and disease [9]. Inflammatory chemokines are induced by infection either directly after innate immune receptor recognition of microbial molecules or indirectly via cytokines secreted in response to infection. Among these cytokines, we have previously described a major role for interferon (IFN)-γ in the neuropathogenesis of experimental African trypanosomiasis. IFN-γ controls parasitemia but paradoxically facilitates the penetration of T cells across the blood-brain barrier into the brain [6] .

Although an association between levels of a few selected chemokines in the CSF and severity of disease in HAT has been described [10, 11], a systematic analysis of chemokine and chemokine receptor expression during trypanosome infections has not been performed. In this study, we have performed a systematic comparison of the expression of chemokines and chemokine receptors in brains from mice before and after parasite passage across the blood-brain barrier and investigated the role played by chemokines during the encephalitic phase of African trypanosomiasis by using relevant knockout mice.

Our results show that CXCL10 is a highly up-regulated chemokine in astrocytes in mice brains after parasite passage across the blood-brain barrier, is induced by IFN-γ and IFN-α/β, facilitates parasite and T cell accumulation in the brain, and accounts at least in part for morbidity. Furthermore, elevated levels of CXCL10 are detected in the CSF of patients with late stage HAT and are associated with low body weight, somnolence, and the presence of trypanosomes within the CSF. We thereby identified CXCL10 as a main regulator in the pathogenesis of African trypanosomiasis as well as a candidate marker of late stage disease.

Table 1. Differential Gene Expression of Chemokine Ligands and Receptors in Mice Brains at Different Time Points after *Trypanosoma brucei brucei* Infection, Determined by Complementary DNA Microarrays

	Fold change in expression	
Chemokine	From 6 to 15 days after infection	From 6 to 28 days after infection
CXC ligand		
CXCL1	…	1.79
CXCL5	…	1.90
CXCL9	…	6.23
CXCL10	2.05	9.94
CXCL12	…	1.35
CXCL13	…	5.08
CXCL14	…	…
CXCL16	…	1.89
CC ligand		
CCL2	…	2.19
CCL4	…	1.70
CCL5	…	4.03
CCL7	…	1.46
CCL9	…	1.48
CCL12	…	2.33
CCL19	…	−2.46
CCL28	1.82	4.17
Chemokine receptor		
CXC receptor		
CXCR4	…	2.08
CXCR6	…	1.87
CX_3C receptor: CX_3CR1	…	2.80
CC receptor		
CCR1	…	1.47
CCR2	…	1.74
CCR3	…	−1.79
CCR5	…	1.57

MATERIALS AND METHODS

Patients and specimens. Patients with early and late stage HAT were recruited from the area around Dipumba Hospital, Mbuji Mayi, Democratic Republic of Congo, where sleeping sickness due to *Trypanosoma brucei gambiense* is endemic. Persons who were seropositive in the card agglutination test for Trypanosomiasis [12] or who presented with suggestive clinical signs were examined for trypanosomes in the blood by capillary tube centrifugation or mini anion exchange centrifugation technique in lymph node aspirate by direct examination and in CSF specimens by modified single centrifugation [13]. The late stage disease was defined as either white blood cell count >5 cells/μL in CSF specimens, counted in disposable counting chambers, or detection of trypanosomes in CSF specimens. The study protocol was approved by the Ministry of Health, Kinshasa, Democratic Republic of Congo, and the Ethical Committee of the University Hospital of Antwerp, Belgium. Patients who were aged <12 years, were moribund, or had "blood-contaminated" CSF were excluded from this study. Somnolence, as determined by the clinician, was defined with sleepiness rating of $\geqslant$5 on the Stanford Sleepiness Scale.

Mice, parasites, and infection. Mice deficient in IFN-g [14], IFN-α/β receptor [15], CXCR3 [16], or CXCL10 [17] were generated by homologous recombination in embryonic stem cells. All strains were back-crossed to a C57BL/6 background, and C57BL/6 mice were used as controls. All experiments were authorized by the local animal research ethical committee. Mice (aged 8–12 weeks; 8–10 mice per group), were infected intraperitoneally with 2×10^3 to 3×10^3 parasites of a pleomorphic stabilate of *T. brucei brucei*, AnTat 1.1E.

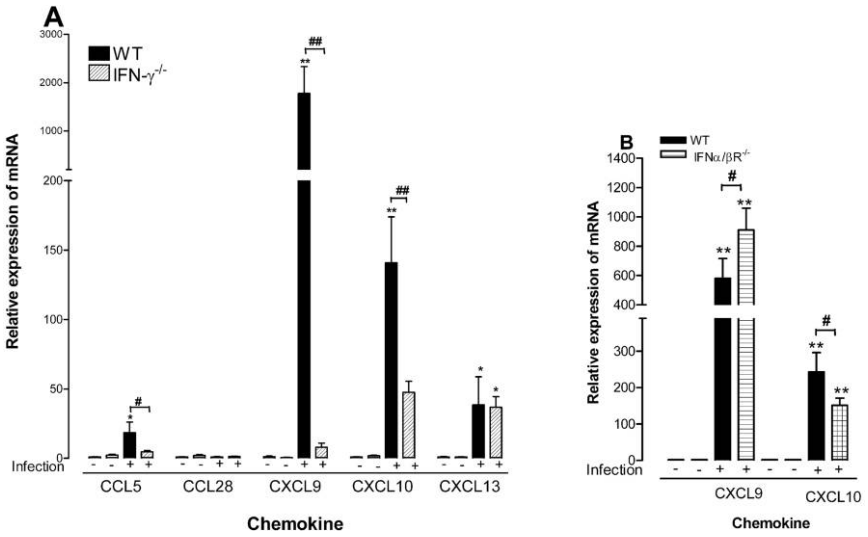

Figure 1. *A,* Relative expression of CCL5, CCL28, CXCL9, CXCL10, and CXCL13 messenger RNA (mRNA) in brains of wild-type and interferon (IFN)-g$^{-/-}$ uninfected (control) and infected mice. Each bar represents the mean (± standard error) of values obtained from 4 animals. *$P < .05$ and **$P < .01$ for the comparison with uninfected wild-type animals; $^{\#}P < .05$ and $^{\#\#}P < .01$ (by 1-way analysis of variance) for the comparison between wild-type and IFN-g$^{-/-}$ infected mice sacrificed at 20 days after infection. *B,* Relative expression of CXCL9 and CXCL10 mRNA in brains of infected wild-type and IFN-a/b receptor (IFN-a/bR)$^{-/-}$ uninfected (control) and infected mice. Each bar represents the mean (± standard error) of values obtained from 4 animals. **$P < .01$ for comparison with uninfected wild-type animals; $^{\#}P < .05$ (1-way analysis of variance) for the comparison of wild-type and IFN-a/bR$^{-/-}$ infected mice sacrificed at 30 days after infection.

Complementary DNA (cDNA) microarray analysis. A transcriptome analysis of total RNA obtained from brains of mice sacrificed before or after parasite penetration into the brain parenchyma was performed as described elsewhere [18].

Real-time reverse-transcriptase polymerase chain reaction (RT-PCR). Gene transcripts of several chemokines were quantified in brains from wild-type, IFN-g$^{-/-}$, IFN-α/β receptor$^{-/-}$ and CXCL10$^{-/-}$ uninfected and infected mice by real-time RT-PCR as described elsewhere [7]. The following primers were used: cyclophilin, sequence described elsewhere [7]; sense CCL5, 5'-CTCGGTCCTGGGAAAATGG-3'; antisense CCL5, 5'-TGCTGATTTCTTGGGTTTGCT-3'; sense CCL28, 5'-GAAGCGCATGGAGCTCTGA-3'; antisense CCL28, 5'-AGCTAGGTGGATCTCTGTGAGTTTG-3'; sense CXCL9, 5'-GCCATGAAGTCCGCTGTTCT-3'; antisense CXCL9, 5'-GGGTTCCTCGAACTCCACACT-3'; sense CXCL10, 5'-GACGGTCCGCTGCAACTG-3'; antisense CXCL10 5'-GCTTCCCTATGGCCCTCATT-3'; sense CXCL11, 5'-GCCCTGGCTGCGATCAT-3'; and antisense CXCL11, 5'-ACAGCGCCCCTGTTTGAA-3'.

Immunohistochemical techniques. To examine passage of trypanosomes across the blood-brain barrier, sections of nonperfused, fresh, frozen brains at a level of the lateral ventricles containing the choroid plexus and septal nuclei were cut, mounted, fixed, and immunostained with either anti-AnTat 1.1 VSG, anti-CD4, or anti-CD8 to determine parasites or T cell presence together with anti-glucose transporter 1 labeling brain endothelial cells as described elsewhere [6]. Microglia and astrocytes were visualized by labeling with anti-Iba1 and anti-GFAP antibodies respectively. The CXCL10 double immunofluorescence staining with GFAP, IbaI, CD4, and CD3 was performed as described elsewhere [19]. Some of the sections were counterstained with DAPI nuclear staining. To determine whether there was neurodegeneration in infected mice, brain sections were stained with β-amyloid precursor protein as described elsewhere [20].

In situ hybridization. The in situ hybridization technique to detect CXCL10 messenger RNA (mRNA) accumulation in the brains of *T. brucei*–infected mice was performed as described elsewhere [19].

Measurement of cytokines/chemokines in CSF of patients with HAT. The levels of IFN-γ and CXCL10 were determined in CSF samples of 20 patients with stage 1 HAT, 20 patients with stage II HAT, and 20 uninfected individuals. The concentration of CXCL10 was determined using a Quantikine human CXCL10 kit (R&D Systems) with a detection limit of 8 pg/mL. IFN-γ levels were measured using a solid phase sandwich enzyme-linked immunosorbent assay (ELISA) (OptiEIA; BD-Pharmingen) with a detection limit of 5 pg/mL.

RESULTS

Identification and regulation of chemokine mRNA levels in the brain of* T. brucei brucei*-infected mice. To define which chemokines are differentially expressed during the encephalitic

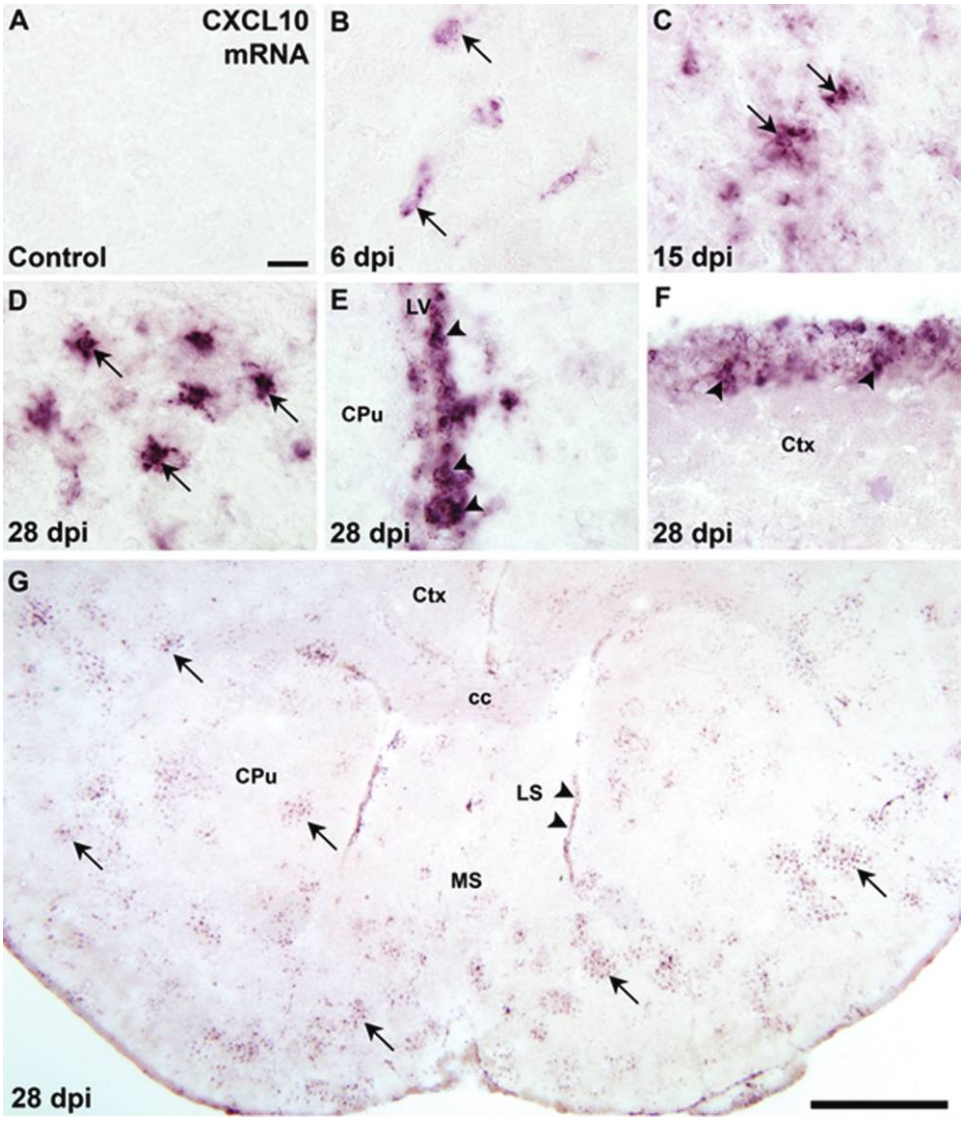

Figure 2. CXCL10 messenger RNA (mRNA)–positive cells in brains of *Trypanosoma brucei brucei*–infected wild-type mice, visualized by an in situ hybridization technique. *A–D,* CXCL10 mRNA was undetectable in uninfected mice *(A)* but was up-regulated in blood vessel–associated cells *(arrows)* at 6 days post infection (dpi) *(B)* and in patches of parenchymal glial-like cells *(arrows)* at 15 *(C)* and at 28 dpi *(D).* The micrographs shown in panels *A–D* were obtained from the ventral part of the brain. *E* and *F,* Ependymal cells *(arrowheads; E)* and meningeal cells *(arrowheads; F)* also expressed CXCL10 mRNA at 6–28 dpi. *G,* Overview showing the patches of CXCL10 mRNA–positive cells *(arrows)* and ependymal cells *(arrowheads)* in a frontal brain section obtained at 28 dpi. Scale bars represent 10 μm in panels *A–F* and 500 μm in panel *G.* cc, corpus callosum; CPu, Caudo- putamen; Ctx, Cortex; LS, Lateral septum; MS, medial septum.

phase of experimental African trypanosomiasis, we compared transcript levels in brain tissues of *T. brucei brucei*–infected mice harvested at 3 different times after infection with use of a high density microarray. Trypanosomes are located within the hemolymphatic system at 6 days after infection; at 15 days after infection, few parasites have penetrated into the brain parenchyma, whereas numerous trypanosomes are present in the brain parenchyma at 28 days after infection. The levels of several chemokine and chemokine receptor transcripts were higher at 28 days than at 6 days after infection (Table 1). Among these, CXCL10, CXCL9, CXCL13, and CCL5 and CCL28 mRNA showed the highest increase ratio. The enhanced expression of chemokine transcripts in infected wild-type mice was confirmed by real-time RT-PCR for all chemokines except CCL28 (Figure 1*A*).

IFN-γ and IFN-α/β have been reported to regulate the expression of CXCL9 and CXCL10 [21–23]. In line with this, CXCL9 and CXCL10 mRNA levels were reduced in brains of IFN-$\gamma^{-/-}$ infected mice, compared with wild-type infected control mice, at 20 days after infection (Figure 1*A*). On the other

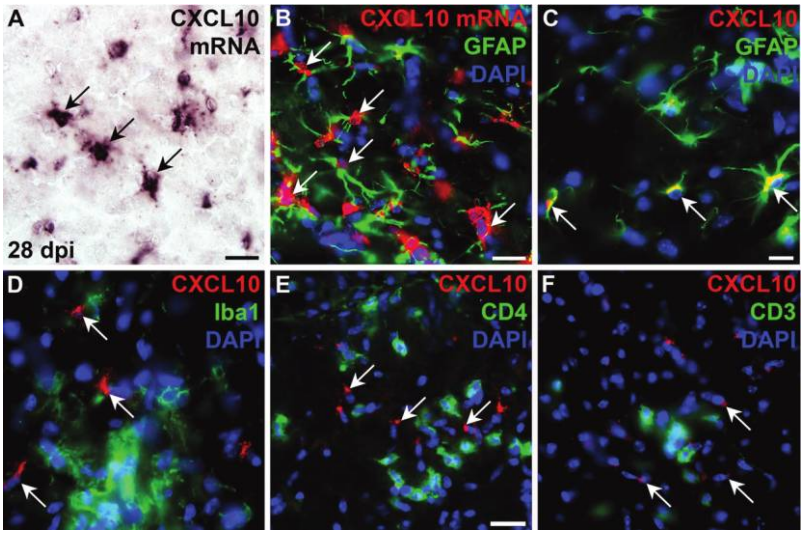

Figure 3. Cellular localization of CXCL10 messenger RNA (mRNA) and CXCL10 in *Trypanosoma brucei brucei*–infected wild-type mice at 28 days post infection (dpi). *A* and *B,* CXCL10 mRNA is expressed in the brain by cells with glial-like morphology *(arrow; A)* and appears to localize to GFAP-positive astrocytes *(arrows)* at 28 dpi *(B). C* and *D,* CXCL10 localizes to GFAP-positive astrocytes *(arrows; C),* whereas Iba1-positive microglia/macrophages did not coexpress CXCL10 *(arrows; D). E* and *F,* The CXCL10-positive astrocytes *(arrows)* surrounded aggregates of $CD4^+$ *(E)* and $CD3^+$ *(F)* T cells . Scale bars represent 10 μm in panels *A* and *B,* 5 μm in panels *C* and *D,* and 20 μm in panels *E* and *F.*

hand, CXCL10 but not CXCL9 mRNA levels were slightly reduced in brains of infected IFN-a/b $receptor^{-/-}$ mice, compared with wild-type mice, at 30 days after infection (Figure 1*B*).

Topological and cellular localization of CXCL10 expression. First, we performed in situ hybridization on mice brain sections to investigate whether CXCL10 mRNA expression varied during the course of *T. brucei brucei* infection. Interestingly, there was a progressive increase in CXCL10 mRNA levels in the brains of infected mice at 6 ($n = 4$), 15 ($n = 3$), and 28 ($n = 3$) days after infection (Figure 2*B*–2*G*), but CXCL10 mRNA was absent in brains of uninfected mice ($n = 4$; Figure 2*A*). Although the CXCL10 mRNA was expressed mainly in blood vessel–associated cells at 6 days after infection (Figure 2*B*), most of the vessel-associated CXCL10 mRNA–positive cells had disappeared, and instead, clusters of mRNA–positive glial-like cells expressing high levels of CXCL10 became visible in the brain parenchyma at 15 days after infection (Figure 2*C*). Clusters were specially observed in the hypothalamus, the optic chiasm, and the optic tracts. At 28 days after infection, clusters of CXCL10 mRNA–positive cells with distinct glial morphology were widely distributed in both hemispheres, including the septal nuclei, caudate putamen, corpus callosum, and cerebral cortex (Figure 2*D*). The CXCL10 mRNA–positive cells appeared to be more evenly distributed within the corpus callosum, optic chiasm, and optic tracts, compared with cells in the grey matter. Ependymal and meningeal cells contained increasing levels of CXCL10 mRNA as infection progressed (Figure 2*E* and 2*F*).

Next, the identity of the CXCL10 mRNA–positive cells (Figure 3*A*) was determined by combining in situ hybridization with immunohistochemistry. CXCL10 mRNA staining was localized in GFAP-negative cells within the blood vessels at 6 days after infection (data not shown) and was colocalized with GFAP-positive astrocytes at 15 and 28 days after infection (Figure 3*B*). Few CXCL10-positive cells were detected at 6 days after infection by labeling with anti-chemokine antibodies (data not shown). In agreement with observations made in CXCL10 mRNA–positive cells, increasing numbers of CXCL10-positive cells were noted in clusters at 15 and 28 days after infection. CXCL10 protein was localized in GFAP-positive astrocytes (Figure 3*C*) but was not found in Iba1-positive microglia (Figure 3*D*) or in $CD4^+$ and $CD3^+$ T cells (Figure 3*E* and 3*F*). At 28 days after infection, the CXCL10-positive astrocytes were localized in inflammatory foci containing Iba1-positive microglia and $CD3^+$ and $CD4^+$ T cells (Figure 3*D*–3*F*). This observation was based on assessment of 4–8 sections from 3 mice per investigated time point.

Role of CXCR3 and CCL10 in the outcome of* T. brucei brucei *infection. IFN-g increases neuroinvasion of trypanosomes and T cells [6]. Because IFN-g–inducible CXCL10 mRNA levels were increased during the late stage of *T. brucei brucei* infection, the role of CXCL10 and its receptor CXCR3 [24, 25] in the outcome of the infection was investigated. Whereas wild-type mice inoculated with *T. brucei brucei* showed significant loss of weight, infected $CXCL10^{-/-}$ and $CXCR3^{-/-}$ mice showed no weight loss during the observation period (Figure 4*A*). Similar parasitemia levels were registered in mutant and wild-type mice (Figure 4*B*).

Next, we studied whether the reduced morbidity observed

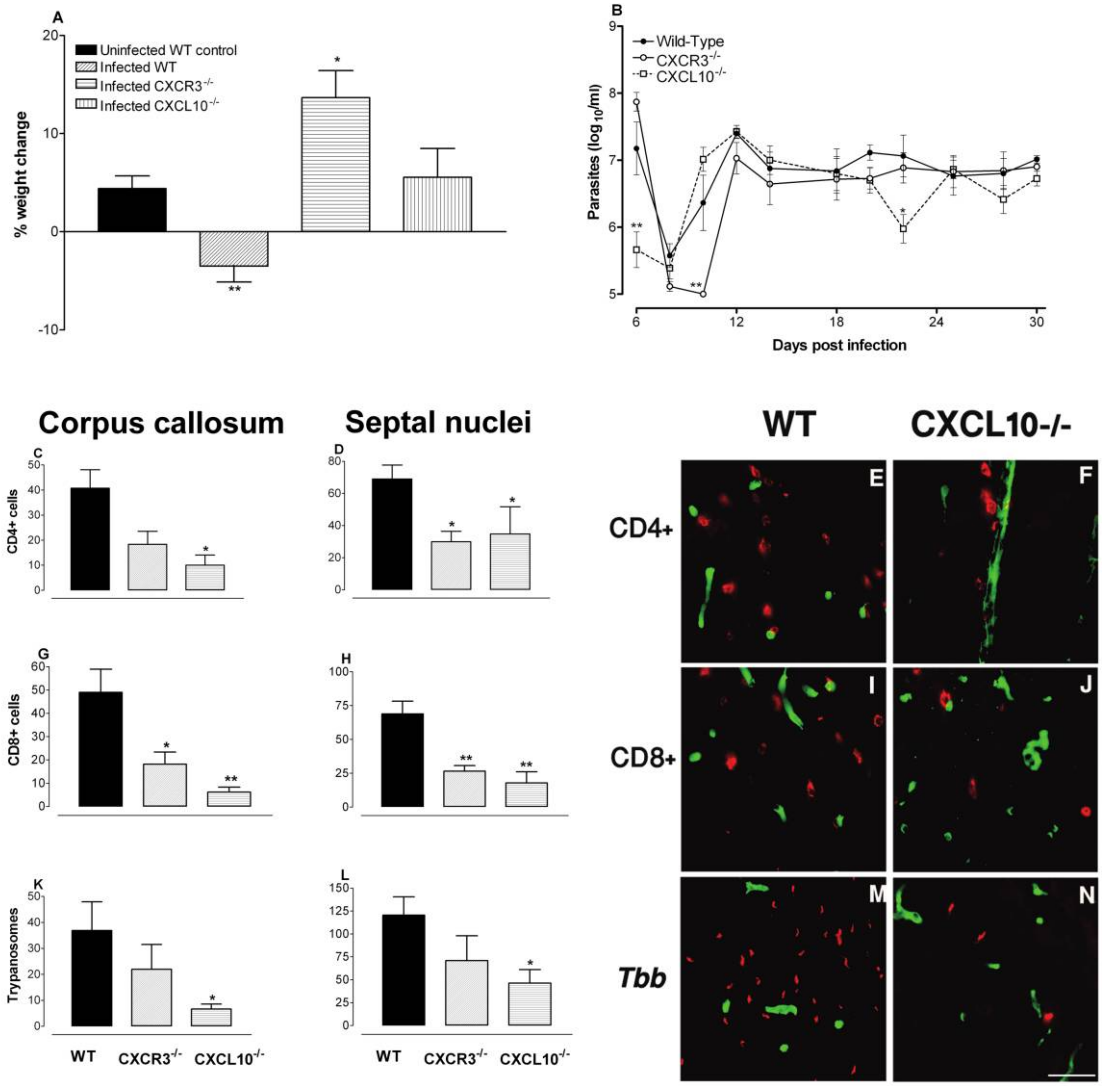

Figure 4. Body weight, parasitemia, CD4+ and CD8+ T cells, and trypanosome accumulation in the brain parenchyma of infected wild-type , CXCR3$^{-/-}$, and CXCL10$^{-/-}$ mice. *A,* Body weight in uninfected wild-type and infected wild-type, CXCR3$^{-/-}$, and CXCL10$^{-/-}$ mice at 30 days after infection. The mean ($\pm$ standard error) weight relative to preinfection weight at day 0, obtained from 6–8 animals, is depicted. *$P < .05$ and **$P < .01$ (by Mann-Whitney *U* test) for comparison with uninfected wild-type animals. *B,* Levels of parasitemia in infected wild-type , CXCR3$^{-/-}$, and CXCL10$^{-/-}$ mice. Each point represents the mean $\log_{10}$ parasites per mL ($\pm$ standard error) obtained for 6–8 animals per group. *$P < .05$ and **$P < .01$ (by 2-way analysis of variance) for comparison with infected wild-type animals. The mean number of CD4$^+$ T cells *(C* and *D),* CD8$^+$ T cells *(G* and *H),* and *Trypanosoma brucei brucei (K* and *L)* per mm^2 in the corpus callosum and septal nuclei of infected wild-type , CXCR3$^{-/-}$, and CXCL10$^{-/-}$ mice at 30 days after infection ($\pm$ standard error) for 6–8 animals per group is depicted. *$P < .05$ and **$P < .01$ (by Mann-Whitney *U* test) for the comparison with wild-type mice at the same time point after infection. *E, F, I, J, M,* and *N,* Immunofluorescent images from the corpus callosum (CD4$^+$ cells, CD8$^+$ cells, *Trypanosoma brucei brucei [red],* and cerebral endothelial cells *[green]*) of infected wild-type and CXCL10$^{-/-}$ mice at 30 days after infection. *E* and *F,* CD4$^+$ cells; *I* and *J,* CD8$^+$ cells; *M* and *N, T. brucei brucei*. In wild-type mice, numerous CD4$^+$ and CD8$^+$ cells and parasites (*E, I,* and *M,* respectively) are observed in the parenchyma. Note the decreased density of CD4$^+$ and CD8$^+$ cells and parasites in the parenchyma of CXCL10$^{-/-}$ mice, compared with wild-type mice *(D, H,* and *M).* The scale bar represents 50 μm.

for infected CXCL10$^{-/-}$ and CXCR3$^{-/-}$ mice could be related to decreased numbers of T cells or parasites in the brain parenchyma. A reduced density of CD4+ and CD8+ T cells in the corpus callosum and septal nuclei of CXCL10$^{-/-}$ and CXCR3$^{-/-}$ mice at 30 days after infection, compared with infected wild-type mice, was observed by double immunolabeling of T cells and cerebral endothelial cells (Figure 4*C*–4*J*). The density of trypanosomes in the parenchyma of the septal nuclei and corpus callosum was significantly reduced in CXCL10$^{-/-}$ mice at 30 days after infection, whereas CXCR3$^{-/-}$ mice showed a reduced accumulation of parasites that failed to reach statistical significance, compared with infected wild-type mice (Fig-

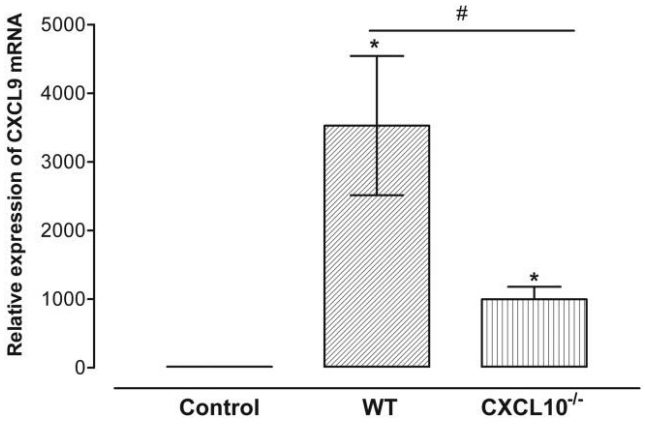

Figure 5. Relative expression of CXCL9 messenger RNA (mRNA) in brains of uninfected and infected wild-type and CXCL10$^{-/-}$ mice. Each bar represents the mean ($\pm$ standard error) of values obtained from 4 animals. *$P < .05$ for the comparison with uninfected wild-type animals; #$P < .05$ (by Mann-Whitney *U* test) for the comparison between wild-type and CXCL10$^{-/-}$ infected mice sacrificed at 30 days after infection.

ure 4*K*–4*N*). The invading trypanosomes were scattered in the brain parenchyma of mutant and wild-type mice (Figure 4*M* and 4*N*). There was no cuffing of trypanosomes or T cells around blood vessels in CXCL10$^{-/-}$ or CXCR3$^{-/-}$ mice as we had previously described in IFN-$\gamma^{-/-}$ and IFN-γ receptor$^{-/-}$ mice [6]. Trypanosomes and CD4+ or CD8+ cells did not colocalize in the brain parenchyma (data not shown). High and similar numbers of trypanosomes and T cells were found in the choroid plexus of infected CXCL10$^{-/-}$, CXCR3$^{-/-}$, and wild-type mice (data not shown).

Similar activation of astrocyte and microglia- as visualized by GFAP and Iba-1 immunolabeling was observed in the corpus callosum and septal nuclei of infected wild-type , CXCL10$^{-/-}$, or CXCR3$^{-/-}$ mice (data not shown). No signs of neurodegeneration were observed in either wild-type , CXCL10$^{-/-}$, or CXCR3$^{-/-}$ infected mice with use of immunolabeling of the β-amyloid precursor protein (data not shown).

Because CXCR3 is also the receptor for CXCL9 [25], we studied whether the absence of CXCL10 affected the levels of CXCL9 mRNA in the brains of mice infected with *T. brucei brucei* at 30 days after infection. Infected CXCL10$^{-/-}$ mice demonstrated reduced levels of CXCL9 mRNA, compared with infected wild-type mice (Figure 5).

Levels of CXCL10 are increased in the CSF of patients with HAT and are associated with severity of the disease. We next investigated whether the increased levels of CXCL10 observed during late-stage experimental African trypanosomiasis is reflected in the human disease. The concentration of CXCL10 in CSF of patients from Democratic Republic of Congo with early-stage ($n = 20$) and late-stage ($n = 20$) HAT caused by *T. brucei gambiense* were measured by ELISA. The titers of CXCL10 in the CSF of patients with late-stage HAT were significantly higher, compared with patients in the early stage of infection and control individuals (Figure 6*A*). Patients in the early stage of infection and uninfected controls had similar levels of CXCL10 (Figure 6*A*). CSF samples from patients with late-stage infection also demonstrated higher levels of IFN-g, compared with patients with early-stage infection (Figure 6*B*).

Increased levels of CXCL10 were associated with increased somnolence, decreased body weight and higher number of trypanosomes in the CSF, but not in the blood, within the late stage patients (Figure 6*C*–6*F*). The concentration of CXCL10 in patients with late-stage infection was not related to age or sex.

DISCUSSION

This study shows that CXCL10 plays an important role in enhancing neuroinflammation in *T. brucei brucei*–infected mice and proposes that CXCL10 could be considered to be a candidate marker for late-stage HAT. Together with CXCL10, CXCL9 and CXCL11 bind to CXCR3, which is expressed on activated T cells, Natural Killer cells, and monocytes/macrophages [25, 26]. CD8$^+$ T cell levels are reduced in brains of lymphocytic choriomeningitis virus (LCMV)–infected CXCL10$^{-/-}$ and CXCR3$^{-/-}$ mice [27, 28], and CD4+ T cell levels are reduced in brains of mouse hepatitis virus–infected mice treated with anti-CXCR3 antibodies [29]; we observed a reduction of both T cells populations in the brains of trypanosome-infected CXCL10$^{-/-}$ and CXCR3$^{-/-}$ mice, compared with wild-type mice.

CXCL9 and CXCL10 gene transcripts are strongly expressed in a mouse model of cerebral malaria, and CXCR3$^{-/-}$ malaria-infected mice have reduced numbers of CD8$^+$ T cells in the brain [30, 31]. Similar to LCMV and malaria infections, morbidity was reduced among *T. brucei brucei*–infected CXCL10$^{-/-}$ and CXCR3$^{-/-}$ mice. However, striking differences in the distribution

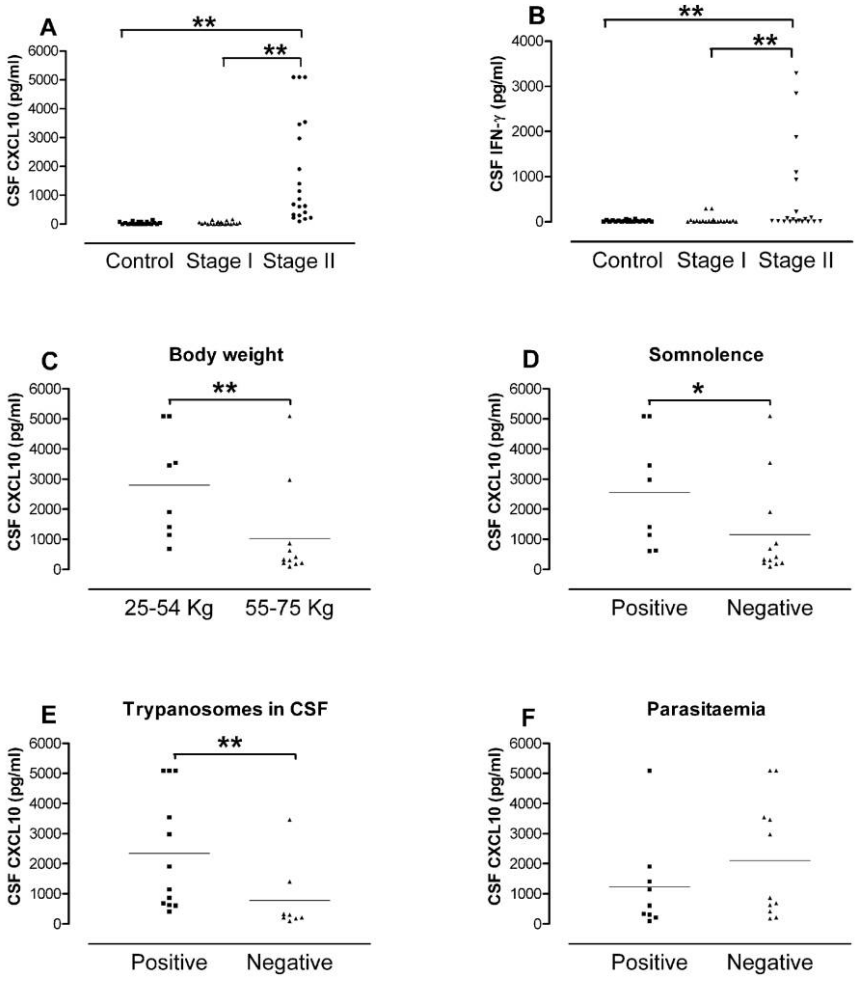

Figure 6. Scatter diagram of concentration of CXCL10 *(A)* and IFN-g *(B)* in the cerebrospinal fluid (CSF) of early- and late-stage patients with human African trypanosomiasis (HAT) and control subjects. $^{**}P < .01$ (by Mann-Whitney *U* test) for the comparison with patients with early-stage HAT and control subjects. *C–F,* CXCL10 in the CSF of patients with late-stage HAT grouped according to their body weight *(C),* somnolence *(D),* presence of trypanosomes in the CSF *(E),* and parasitemia *(F).* The mean CXCL10 concentration per group is depicted. $^{*}P < .05$ and $^{**}P < .01$ (by Mann-Whitney *U* test) for differences in CXCL10 levels between patients with low weight and normal weight *(C),* between patients positive and negative for somnolence *(D),* or between patients with trypanosomes in CSF *(E).*

of the T cells in the brain during *T. brucei brucei,* LCMV, and *Plasmodium falciparum* infections can be noted despite the fact that CXCL10 is strongly up-regulated in all 3 disease models. Whereas widely scattered $CD4^+$ and $CD8^+$ T cells predominate in hypothalamic areas, septal nuclei, and white matter in *T. brucei brucei*–infected mice, $CD8^+$ T cells are observed around the surfaces of the ventricular system as well as in the major white matter tracts in LCMV-infected mice. In *P. falciparum*–infected mice, $CD8^+$ T cells are, on the other hand, sequestered within cerebral vessels in various brain regions and do not infiltrate the parenchyma. The T cells in these 3 different infections, therefore, demonstrate a topological localization in the brain that is similar to that of the pathogens.

The spatial-temporal expression profile of CXCL10 seemed to mirror the course of the trypanosome infection in the brain. During the hemolymphatic stage of the disease, 6 days after infection in our mouse model, CXCL10 was found in cells of the choroid plexus and in cells associated with cerebral blood vessels with a widespread distribution in the brain. However, later during the course of the disease, when trypanosomes were observed in brain parenchyma in addition to the choroid plexus, CXCL10 expression was up-regulated not only in meningeal and ependymal cells but also in astrocytes, which appeared to cluster around vessels in regions of the brain showing T cell infiltration. Astrocyte activation has previously been implicated in the pathobiology of African trypanosomiasis [32, 33]. In accordance, CXCR3 signaling has been suggested to constrain $CD4^+$ T cells to perivascular spaces in an experimental allergic encephalomyelitis model [34]. Also in such a model, the central nervous system expression of the CXCL10 gene

occurred predominantly in parenchymal astrocytes that surrounded inflammatory lesions [35].

In our African trypanosomiasis disease model, CXCL10 was up-regulated in parenchymal astrocytes of hypothalamic regions, optic chiasm, and optic tracts when trypanosomes [36] and T cells [37] have infiltrated and IL-1, TNF-α, and IFN-g mRNAs have been induced [38] in the nearby circumventricular organs and choroid plexus for an extended period of time. It could therefore be speculated that, over time, cytokines produced in these areas may leak through their surrounding barriers and the choroid plexus epithelia into the CSF to induce CXCL10 production in ependymal and meningeal cells and between ependymal cells into the brain parenchyma [39], to induce chemokine production in astrocytes as observed by others [40]. The CXCL10 expression in perivascular astrocytes may facilitate the passage of T cells accompanied by the parasites across the blood-brain barrier to these areas of the brain. The infiltrating T cells would then augment the process by secreting IFN-g, which in turn induces more widespread expression of CXCL10 [6].

We have previously observed that the passage of trypanosomes across the blood-brain barrier, which occurs at a late stage of infection, is a multistep process similar to that of leukocytes [6]. Although the endothelial basement membrane is permissive to parasite penetration, modifications of the astrocytic basement membrane by IFN-g–dependent factors are required to permit trypanosome passage. In the absence of IFN-γ, trypanosomes are trapped between the basement membranes, forming cuffs [6]. Such cuffing of trypanosomes around vessels was not observed in CXCL10$^{-/-}$ or CXCR3$^{-/-}$ mice, which demonstrates that CXCL10 is not involved in facilitating the passage of trypanosomes across the astrocytic basement membrane but could play a role by increasing the trafficking of both leukocytes and trypanosomes over the cerebral endothelial cells or by increasing their retention in the brain parenchyma. The distribution of inflammatory cells and trypanosomes in CXCR3$^{-/-}$, CXCL10$^{-/-}$, and IFN-$\gamma^{-/-}$ mice therefore suggests the involvement of different IFN-γ–regulated genes in cerebral penetration of leukocytes and parasites.

Similar to that observed for LCMV infection [28] and in the experimental allergic encephalomyelitis model [9], we observed diminished levels of CXCL9 mRNA in brains of *T. brucei brucei*–infected CXCL10$^{-/-}$ mice. CXCL9 production is induced by IFN-g [23]. The reduction in CXCL9 transcripts observed in *T. brucei brucei*–infected CXCL10$^{-/-}$ mice, compared with wild-type mice, is therefore most likely attributable to the reduced T cell accumulation in the brain that results in less IFN-g production in knockout mice. CXCL11 is also a high affinity ligand for CXCR3; however, in the C57BL6 mouse strain CXCL11 it is likely nonfunctional as a result of a single point mutation that deletes a nucleotide base within the coding sequence of the CXCL11 gene [35]. Of interest, IFN-α/β also seemed to play a role in the increased CXCL10 but not CXCL9 mRNA levels during the late phase of *T. brucei brucei* infection. The regulation of CXCL10 by IFN-α/β has been shown in other experimental systems [22], but the role of IFN-α/β, a family of important immunoregulatory cytokines, has not been studied in detail, particularly during the early stages of infection with *T. brucei brucei*.

Although drugs for treatment of the early stage of HAT are efficient, many, if not most, patients seek medical advice only when reaching the meningoencephalitic stage, for which toxic arsenic compounds are widely used. Better diagnostic markers are needed to distinguish the 2 stages of infection; presently, this distinction relies on the finding of increased numbers of leukocytes and/or trypanosomes in the CSF and/or detectable levels of intrathecal immunoglobulin M. It has been shown that levels of CXCL8, CCL2, and CCL3 [10, 11] in the CSF associate with disease severity in patients with HAT. Concentrations of IFN-γ in CSF and/or plasma of patients with late-stage HAT have also been associated with disease severity [41]. The detection of CXCL10 mRNA in the mouse brain after trypanosomes had crossed the blood-brain barrier suggested that this molecule could also be an interesting candidate to distinguish between the stages before and after parasites have invaded the brain patients with HAT. In fact, high levels of CXCL10 were found in the CSF of patients with late-stage HAT, whereas none of the patients with early-stage HAT demonstrated increased concentrations of the chemokine. Levels of CXCL10 were associated with the degree of somnolence and loss of body weight. The presence of trypanosomes in the CSF but not in blood was also associated with increased levels of CXCL10 in the CSF, altogether suggesting that CXCL10 could be considered to be a new candidate marker to be further evaluated for determining the stage of disease. In line with our results, it has been recently reported that, of 13 cytokines/chemokines screened in the CSF, CXCL10 seemed to best distinguish between early- and late-stage HAT [42].

In conclusion, we identified CXCL10 as an IFN-γ–regulated chemokine that is robustly increased at late stages of infection with African trypanosomes in humans and mice. Binding of CXCL10 to CXCR3 facilitates T cell and parasite accumulation in the brain parenchyma during murine trypanosomiasis and plays an important role in the morbidity observed in the late stage of the infection.

References

1. Chappuis F, Loutan L, Simarro P, Lejon V, Buscher P. Options for field diagnosis of human african trypanosomiasis. Clin Microbiol Rev **2005**; 18:133–46.
2. WHO. Control and surveillance of African trypanosomiasis. Report of a WHO Expert Committee. World Health Organ Tech Rep Ser **1998**; 881:I-VI, 1–114.

3. Lejon V, Reiber H, Legros D, et al. Intrathecal immune response pattern for improved diagnosis of central nervous system involvement in trypanosomiasis. J Infect Dis **2003**; 187:1475–83.
4. Kennedy PG. Human African trypanosomiasis of the CNS: current issues and challenges. J Clin Invest **2004**; 113:496–504.
5. Mulenga C, Mhlanga JD, Kristensson K and Robertson B. *Trypanosoma brucei brucei* crosses the blood-brain barrier while tight junction proteins are preserved in a rat chronic disease model. Neuropathol Appl Neurobiol **2001**; 27:77–85.
6. Masocha W, Robertson B, Rottenberg ME, Mhlanga J, Sorokin L, Kristensson K. Cerebral vessel laminins and IFN-γ define *Trypanosoma brucei brucei* penetration of the blood-brain barrier. J Clin Invest **2004**; 114:689–94.
7. Masocha W, Rottenberg ME, Kristensson K. Minocycline impedes African trypanosome invasion of the brain in a murine model. Antimicrob Agents Chemother **2006**; 50:1798–804.
8. Luster AD. Chemokines—chemotactic cytokines that mediate inflammation. N Engl J Med **1998**; 338:436–45.
9. Klein RS. Regulation of neuroinflammation: the role of CXCL10 in lymphocyte infiltration during autoimmune encephalomyelitis. J Cell Biochem **2004**; 92:213–22.
10. Lejon V, Lardon J, Kenis G, et al. Interleukin (IL)-6, IL-8 and IL-10 in serum and CSF of *Trypanosoma brucei gambiense* sleeping sickness patients before and after treatment. Trans R Soc Trop Med Hyg **2002**;96: 329–33.
11. Courtioux B, Boda C, Vatunga G, et al. A link between chemokine levels and disease severity in human African trypanosomiasis. Int J Parasitol **2006**; 36:1057–65.
12. Magnus E, Lejon V, Bayon D, et al. Evaluation of an EDTA version of CATT/*Trypanosoma brucei gambiense* for serological screening of human blood samples. Acta Trop **2002**; 81:7–12.
13. Büscher P, Lejon V. Diagnosis of human African trypanosomiasis. In: Maudlin I, Holmes P and Miles MA, eds. The trypanosomiases. Oxfordshire: CABI Publishing, **2004**:203–18.
14. Muller U, Steinhoff U, Reis LF, et al. Functional role of type I and type II interferons in antiviral defense. Science **1994**; 264:1918–21.
15. van den Broek MF, Muller U, Huang S, Zinkernagel RM, Aguet M. Immune defence in mice lacking type I and/or type II interferon receptors. Immunol Rev **1995**; 148:5–18.
16. Hancock WW, Gao W, Faia KL, Csizmadia V. Chemokines and their receptors in allograft rejection. Curr Opin Immunol **2000**; 12:511–6.
17. Dufour JH, Dziejman M, Liu MT, Leung JH, Lane TE, Luster AD. IFN-γ-inducible protein 10 (IP-10; CXCL10)-deficient mice reveal a role for IP-10 in effector T cell generation and trafficking. J Immunol **2002**; 168:3195–204.
18. Lindberg J, af Klint E, Catrina AI, et al. Effect of infliximab on mRNA expression profiles in synovial tissue of rheumatoid arthritis patients. Arthritis Res Ther **2006**; 8:R179.
19. Lambertsen KL, Gregersen R, Drojdahl N, Owens T, Finsen B. A specific and sensitive method for visualization of tumor necrosis factor in the murine central nervous system. Brain Res Brain Res Protoc **2001**; 7: 175–91.
20. Mankowski JL, Queen SE, Tarwater PM, Fox KJ, Perry VH. Accumulation of beta-amyloid precursor protein in axons correlates with CNS expression of SIV gp41. J Neuropathol Exp Neurol **2002**; 61:85–90.
21. Vanguri P, Farber JM. Identification of CRG-2. An interferon-inducible mRNA predicted to encode a murine monokine. J Biol Chem **1990**; 265:15049–57.
22. Tebo JM, Kim HS, Gao J, Armstrong DA, Hamilton TA. Interleukin-10 suppresses IP-10 gene transcription by inhibiting the production of class I interferon. Blood **1998**; 92:4742–9.
23. Farber JM. Mig and IP-10: CXC chemokines that target lymphocytes. J Leukoc Biol **1997**; 61:246–57.
24. Weng Y, Siciliano SJ, Waldburger KE, et al. Binding and functional properties of recombinant and endogenous CXCR3 chemokine receptors. J Biol Chem **1998**; 273:18288–91.
25. Loetscher M, Gerber B, Loetscher P, et al. Chemokine receptor specific for IP10 and mig: structure, function, and expression in activated T-lymphocytes. J Exp Med **1996**; 184:963–9.
26. Cole KE, Strick CA, Paradis TJ, et al. Interferon-inducible T cell α chemoattractant (I-TAC): a novel non-ELR CXC chemokine with potent activity on activated T cells through selective high affinity binding to CXCR3. J Exp Med **1998**; 187:2009–21.
27. Christensen JE, Nansen A, Moos T, et al. Efficient T-cell surveillance of the CNS requires expression of the CXC chemokine receptor 3. J Neurosci **2004**; 24:4849–58.
28. Christensen JE, de Lemos C, Moos T, Christensen JP,Thomsen AR. CXCL10 is the key ligand for CXCR3 on $CD8^+$ effector T cells involved in immune surveillance of the lymphocytic choriomeningitis virus–infected central nervous system. J Immunol **2006**; 176:4235–43.
29. Stiles LN, Hosking MP, Edwards RA, Strieter RM and Lane TE. Differential roles for CXCR3 in $CD4^+$ and $CD8^+$ T cell trafficking following viral infection of the CNS. Eur J Immunol **2006**; 36:613–22.
30. Miu J, Mitchell AJ, Muller M, et al. Chemokine gene expression during fatal murine cerebral malaria and protection due to CXCR3 deficiency. J Immunol **2008**; 180:1217–30.
31. Campanella GS, Tager AM, El Khoury JK, et al. Chemokine receptor CXCR3 and its ligands CXCL9 and CXCL10 are required for the development of murine cerebral malaria. Proc Natl Acad Sci U S A **2008**; 105:4814–9.
32. Hunter CA, Gow JW, Kennedy PG, Jennings FW,Murray M. Immunopathology of experimental African sleeping sickness: detection of cytokine mRNA in the brains of *Trypanosoma brucei brucei*–infected mice. Infect Immun **1991**; 59:4636–40.
33. Hunter CA, Jennings FW, Kennedy PG, Murray M. Astrocyte activation correlates with cytokine production in central nervous system of *Trypanosoma brucei brucei*–infected mice. Lab Invest **1992**; 67:635–42.
34. Muller M, Carter SL, Hofer MJ, et al. CXCR3 signaling reduces the severity of experimental autoimmune encephalomyelitis by controlling the parenchymal distribution of effector and regulatory T cells in the central nervous system. J Immunol **2007**; 179:2774–86.
35. Carter SL, Muller M, Manders PM, Campbell IL. Induction of the genes for Cxcl9 and Cxcl10 is dependent on IFN-γ but shows differential cellular expression in experimental autoimmune encephalomyelitis and by astrocytes and microglia in vitro. Glia **2007**; 55:1728–39.
36. Schultzberg M, Ambatsis M, Samuelsson EB, Kristensson K, van Meirvenne N. Spread of *Trypanosoma brucei* to the nervous system: early attack on circumventricular organs and sensory ganglia. J Neurosci Res **1988**; 21:56–61.
37. Schultzberg M, Olsson T, Samuelsson EB, Maehlen J, Kristensson K. Early major histocompatibility complex (MHC) class I antigen induction in hypothalamic supraoptic and paraventricular nuclei in trypanosome-infected rats. J Neuroimmunol **1989**; 24:105–12.
38. Quan N, Mhlanga JD, Whiteside MB, McCoy AN, Kristensson K, Herkenham M. Chronic overexpression of proinflammatory cytokines and histopathology in the brains of rats infected with *Trypanosoma brucei.* J Comp Neurol **1999**; 414:114–30.
39. Brightman MW, Reese TS. Junctions between intimately apposed cell membranes in the vertebrate brain. J Cell Biol **1969**; 40:648–77.
40. Christensen JE, Simonsen S, Fenger C, et al. Fulminant lymphocytic choriomeningitis virus–induced inflammation of the CNS involves a cytokine-chemokine-cytokine-chemokine cascade. J Immunol **2009**; 182:1079–87.
41. Maclean L, Odiit M, Macleod A, et al. Spatially and genetically distinct African trypanosome virulence variants defined by host interferon-γ response. J Infect Dis **2007**; 196:1620–8.
42. Hainard A, Tiberti N, Robin X, et al. A combined CXCL10, CXCL8 and H-FABP panel for the staging of human African trypanosomiasis patients. PLos Negl Trop Dis **2009**; 3:e459.